Published in Microporous and Mesoporous Materials 57, issue 3, 273-282, 2003
which should be used for any reference to this work

The effect of the carbonization/activation procedure on the microporous texture of the subsequent chars and active carbons

Benoît Cagnon [a], Xavier Py [a], André Guillot [a,*], Fritz Stoeckli [b]

[a] *CNRS-IMP, Institut de Science et Génie des Matériaux et Procédés, Rambla de la Thermodynamique, 52 Avenue de Villeneuve, Tecnosud, F-66100 Perpignan Cedex, France*
[b] *Chemistry Department, University of Neuchâtel, Avenue de Bellevaux 51, CH-2000 Neuchâtel, Switzerland*

Abstract

Chars obtained by carbonizing coconut shells at different intermediate heat treatment temperatures (IHTT) between 400 and 800 °C were activated at 800 °C in a stream of $N_2 + H_2O$, following two distinct procedures. In the first procedure, activation follows directly the carbonization, whereas in the second procedure, the sample was first brought back to 25 °C and subsequently heated again to the activation temperature of 800 °C. The data for CO_2 adsorption at 25 °C and N_2 at −196 °C with immersion calorimetry confirms that the activated carbons derived from chars obtained at low IHTT and in two steps, present a ''gate effect'' for burn-offs <20% or 25%, otherwise, the final carbons present similar structural characteristics for higher burn-offs. It also appears that the evolution of the average pore width L_0 with the micropore volume W_0 follows a general pattern outlined early.

Keywords: Chars; Carbonization; Temperature; Activated carbons; Adsorption

1. Introduction

Activated carbons can be prepared from a variety of precursors, but the ones most commonly used are peat, coal, wood and coconut shells [1].

It is well known, that the microporous properties of the resulting activated carbons depend on both the precursor and the conditions of carbonization and activation. Various studies are dealing with the influence of carbonization and the subsequent activation on the microporous properties of carbons derived from lignocellulosic materials [2–5]. Most of these authors believe that the carbonization temperature does not significantly affect the pore structure of the carbonized material, but more recently it has been shown [6] that the development of porosity in palm-shell-based activated carbon strongly depends on the temperature at which the char was prepared.

The main objective of this study was to determine the influence of the intermediate heat treatment temperature (IHTT) of carbonization on the carbon yield, on the properties of the chars and of

* Corresponding author. Tel.: +33-4-68-66-21-10; fax: +33-4-68-68-22-13.
E-mail address: guillot@univ-perp.fr (A. Guillot).

Nomenclature

A	Polanyi adsorption potential ($kJ\,mol^{-1}$)	S_{BET}	BET surface area ($m^2\,g^{-1}$)
E_0	characteristic energy of adsorption ($kJ\,mol^{-1}$)	S_e	external surface area ($m^2\,g^{-1}$)
d	true density ($g\,cm^{-3}$)	T	temperature (°C or K)
h_i	specific enthalpy of wetting ($J\,m^{-2}$)	V_m	molar volume in the adsorbed state ($cm^3\,mmol^{-1}$)
L_0	mean pore size (nm)	W_0	specific micropore volume ($cm^3\,g^{-1}$)
n	exponent of the Dubinin–Astakhov equation (–)	W_t	specific total pore volume (at $p/p_s = 0.95$) ($cm^3\,g^{-1}$)
N_a	specific adsorbed amount ($mol\,kg^{-1}$)	$\Delta_i H$	specific enthalpy of immersion ($J\,g^{-1}$)
N_{ao}	maximum specific adsorbed amount ($mol\,kg^{-1}$)	α	thermal expansion coefficient of the liquids (K^{-1})
p	partial pressure of vapor (kPa)	β	affinity coefficient (–)
p_s	saturation pressure (kPa)	σ	standard deviation of the distribution
R	gas constant ($8.314\ J\,K^{-1}\,mol^{-1}$)	Γ	gamma function (tabulated) (–)

the corresponding activated carbons, as well as the influence of a one- and two-step procedure before activation at 800 °C. To our knowledge, little attention has been paid so far to these factors, which induce structural changes in the chars and in the subsequent activated carbons with burn-offs (relative mass losses) below 20–25%.

2. Theory

As discussed in detail elsewhere, microporous carbons can be characterized within the frame of Dubinin's theory [7–10] and its extension to immersion calorimetry [7,8]. The basic relation is the Dubinin–Astakhov (DA) equation

$$N_a = N_{ao} \exp[-(A/\beta E_0)^n] \quad (1)$$

where N_a represents the amount adsorbed at relative pressure p/p_s, N_{ao} is the limiting amount filling the micropores and $A = RT \ln(p_s/p)$ (where the temperature T is in Kelvin). Exponent $n = 2$ corresponds to the classical Dubinin–Radushkevich (DR) equation, valid for most activated carbons. Parameters β and E_0 depend, respectively, on the adsorptive and on the solid. The experimental affinity coefficients are given in the literature [7,8,11], and in the present study we used $\beta(CO_2) = 0.35$ [12], as confirmed by recent studies [13,14]. It has been shown that in the case where the DR equation applies, the average micropore width L_0 is related to E_0 by

$$L_0 = 10.8/(E_0 - 11.4) \quad (2)$$

The limiting micropore volume $W_0 = N_{ao} V_m$, in which V_m is the molar volume in the adsorbed state (to a first and often good approximation, it is assumed to be that of the corresponding liquid or solid at the given temperature). The external surface S_e and the micropore volume W_0 can also be deduced from the comparison of the experimental adsorption data with a reference isotherm determined under the same conditions on a non-porous material. This approach has the advantage that it does not depend on a theory. The external surface corresponds to the linear section of the comparison plot, usually in the range of relative pressures $0.2–0.3 < p/p_s < 0.7–0.8$, its value is calculated from the slope. The micropore volume is obtained by extrapolating this section to the origin. The method has been applied in the form of the well-known α_s plot proposed by Gregg and Sing [15].

As shown elsewhere [7,8], Eq. (1) leads to an expression for the enthalpy of immersion into the corresponding liquid,

$$\Delta_i H\ (J\,g^{-1}) = -\beta E_0 (W_0/V_m)(1 + \alpha T) \times \Gamma(1 + 1/n) + h_i S_e \quad (3)$$

in which α is the expansion coefficient of the liquid, Γ is the *Gamma* function and $h_i S_e$ represents the wetting of the external (non-microporous) surface area of the solid, S_e. For carbons, h_i is typically around $-0.1\ \mathrm{J\,m^{-2}}$.

With the help of Eq. (3), it is possible to calculate the micropore volume $W_0(L_c)$ actually filled by a molecular probe with a critical dimension L_c, which leads to the micropore size distribution $\Delta W/\Delta L = f(L)$.

Alternatively, it is possible to derive the pore size distribution (PSD) from the adsorption isotherm of a small probe such as CO_2 on the basis of an expression suggested by Stoeckli [8,16] or by using standard isotherms based on computer modeling [13,14]. It has been shown that the two techniques lead to similar PSDs. On the other hand, if "gate effects" are present, the distribution $\Delta W/\Delta L = f(L)$, based on liquid molecular probes, will be different. This has been illustrated by a recent study of molecular-sieve carbons resulting from activated carbons coated with a polymer and subsequently carbonized [17]. Under these circumstances, access to the micropores is reduced by constrictions, a situation also found for chars and carbons with low degrees of activation [18].

3. Materials and experimental techniques

Series of chars and steam-activated carbons were prepared from clean coconut shells, which were crushed and sieved to a particle size of approximately 200 μm. The composition of the raw lignocellulosic material is given in Table 1 (courtesy *Service Central d'Analyse du C.N.R.S* and *CERMAV-CNRS*).

Pyrolysis was carried out in batches of 10 g in a horizontal reactor made of stainless steel and heated in an electric furnace.

In the present study, two distinct procedures, illustrated in Fig. 1a and b, respectively, were used to produce activated carbons.

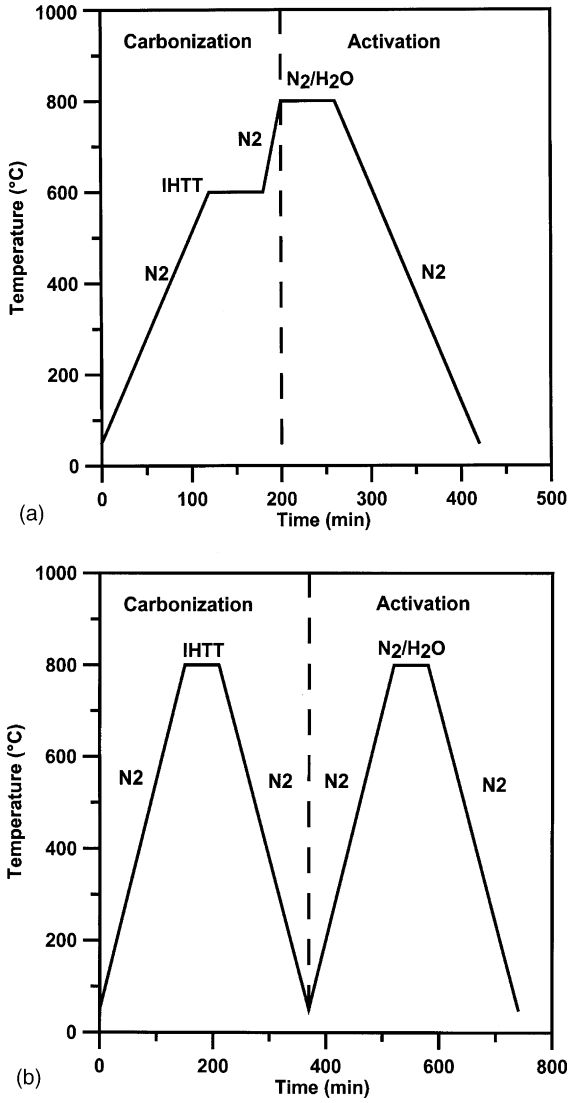

Fig. 1. (a) One-step procedure with IHTT at 600 °C. (b) Two-step procedure with IHTT at 800 °C.

In the first procedure, starting at room temperature and following an initial gradient of 5 °C/min, isothermal heat soaking was carried out for

Table 1
Composition of the raw material (coconut shell)

Hemicellulose (wt.%)	Cellulose (wt.%)	Lignin (wt.%)	C (wt.%)	H (wt.%)	N (wt.%)	O (wt.%)	Ash (wt.%)
35	15	50	48.72	5.78	<0.26	42.53	2.71

1 h at seven different IHTT of 400, 550, 600, 650, 700, 750 and 800 °C, under a nitrogen flow of 1 l/min. Subsequently, the sample was brought into contact with an $N_2 + H_2O$ mixture at 800 °C (Fig. 1a). Therefore, in all cases the chars reach the temperature of 800 °C with a gradient of 10 °C/min and a nitrogen flow of 1 l/min.

The subsequent activation took place in the same furnace, using an $N_2 + H_2O$ flow of 1 l/min, the water vapor being generated from the liquid at 70 °C. Reaction times of 60, 120, 165, 210, 240, 270 min were used to produce carbons with increasing degrees of burn-off (loss weight relative to the char at 800 °C).

In the second procedure, the activation procedure was the same, but after reaching the IHTT and soaking at this temperature for 1 h, the sample was allowed to cool down to room temperature under nitrogen (1 l/min) with a temperature gradient of −10 °C/min (Fig. 1b). The sample was again brought up to 800 °C (5 °C/min), soaked for 1 h and subsequently activated between 60 and 270 min under the same conditions as in the first procedure. Finally, the sample was cooled at a rate of 10 °C/min. The main and fundamental difference with the first procedure is the cooling down to room temperature, followed by a return to 800 °C.

The samples (chars and activated carbons) were characterized by N_2 adsorption at −196 °C with the help of an automated adsorption apparatus (Micromeritics ASAP 2000M). The data was analyzed by using the Dubinin–Radushkevich equation [7,8], where the linear section of the log/log plot leads to the micropore volume W_0 and the characteristic energy E_0. The latter is related to the average micropore width L_0 [8,19]. As mentioned above the α_s-plot leads to a determination of the external surface area S_e and provides a second estimation of W_0 (black carbon Vulcan 3 was taken as reference [20]). The standard BET technique leads to an equivalent surface area. In some cases, CO_2 isotherms were also determined at 25 °C, following a procedure described in detail elsewhere [20]. These isotherms were used to derive PSD [13,14]. As the solids have low external surface areas ($S_e < 20$–25 m^2/g), the total pore volume (W_t) could be estimated directly from the amount adsorbed at relative pressure $p/p_s = 0.95$.

The true densities of the raw materials and the carbons were obtained by pycnometry (*Micromeretics AccuPyc 1330*), using helium at 25 °C as displacement fluid.

The samples were also characterized by immersion calorimetry at 20 °C, as described in detail elsewhere [8]. This approach provides information on the accessible pores from the liquid phase. In the present study, we used mainly CH_2Cl_2 (0.33 nm) and CCl_4 (0.63 nm), which are sufficient to reveal so-called ''gate effects'', as discussed in detail elsewhere [16,17].

The activated carbons are identified by a code corresponding to the overall procedure followed (1 or 2), the IHTT (in °C), the final process (A = activation) and finally the activation time at 800 °C in minutes. For example, 1-650-A-120 is a sample resulting from the one-step method with an IHTT of 650 °C and subsequently activated for 2 h at 800 °C. For the chars, we only use ''C'' for carbonization and the IHTT in °C. Accordingly, C650 is a coconut shell carbonized at 650 °C.

4. Results and discussion

4.1. Effect of IHTT carbonization on the properties of the chars

Table 2 shows the carbon yield during carbonization, defined as the ratio of m_f, the weight of the char, to the weight of the initial raw material m_i (10 g),

$$\text{Yield } (\%) = \frac{m_f}{m_i} \times 100 \tag{4}$$

This quantity decreases from 37.5% to 25.6% with increasing IHTT, the highest mass loss occurring below 550 °C. Between 600 and 800 °C, the solid looses essentially all volatile material. In the case of char C700, the yield value of 29.7 is somewhat higher than for chars C550 to C800, which may reflect a certain inhomogeneity in the starting material. We believe that this deviation has no real significance.

It appears that chars with an IHTT below 700 °C have a true density similar to that of the raw material ($d = 1.450$ g/cm^3), which indicates that

Table 2
Effect of IHTT on the properties of the chars

Sample	Yield (%)	W_t (cm^3/g) (N_2) and (CO_2)	W_0 (cm^3/g) (N_2) and (CO_2)	E_0 (kJ/mol) (N_2)		L_0 (nm) (N_2)		E_0 (kJ/mol) (CO_2)	L_0 (nm) (CO_2)	True density (g/cm^3) (He)[a]
				Adsorption	Desorption	Adsorption	Desorption			
C400	37.5	–	–	–	–	–	–	–	–	1.470
C550	27.6	0.20	0.19	16.7	18.6	2.02	1.49	31.0	0.55	1.474
C600	27.2	0.20	0.20	21.5	23.3	1.07	0.91			1.558
C650	27.2	0.19	0.19	23.9	23.3	0.86	0.91	34.0	0.48	1.611
C700	29.7	0.18	0.18	24.9	27.3	0.80	0.68	31.7	0.53	1.822
C750	26.6	0.19	0.18	24.8	29.3	0.81	0.60			1.790
C800	25.6	0.19	0.18	24.5	31.0	0.83	0.55	35.3	0.47	1.934

[a] The raw material (coconut shell) has a density of 1.450 g/cm^3.

carbonization is not complete. On the other hand, the true density increases with IHTT, and beyond 700 °C it is close to the value of graphite (d = 2.250 g/cm^3). This suggests a relatively dense carbon structure with voids (micropores) accessible to helium. It appears therefore that in the case of coconut shells, carbonization is practically complete at 800 °C.

It is also interesting to examine the influence of IHTT on the microporosity of chars C550 to C800. As shown in Table 2, the micropore volume W_0 obtained with N_2 (−196 °C) and CO_2 (25 °C) and the total pore volume W_t are practically identical for all the chars (≈0.20 cm^3/g). Char C400 does not adsorb nitrogen, but from its helium density, which is very close to that of char C550, one may conclude that the microporosity should also be around 0.20 cm^3/g. The IHTT of 400 °C was therefore abandoned for further treatments.

It also appears that with increasing IHTT, the average micropore width L_0 calculated from the nitrogen desorption isotherms with the help of Eq. (2), tends to decrease from 1.5 to 0.55 nm (as pointed out elsewhere [19], the uncertainty on L_0 is around ±0.05–0.07 nm). Whatever the IHTTs, the values of L_0 obtained from the adsorption branch of the nitrogen isotherms are somewhat higher than those obtained from the desorption branch. This reflects incomplete micropore filling due to "gate effects", which result from tarry materials and lead to activated diffusion. This is confirmed by the values calculated from the CO_2 adsorption isotherms. Furthermore, as seen in Fig. 2, it appears that at the low IHTTs the chars follow the so-called regime III, which is characteristic of underdeveloped porosity [21]. On the other hand, chars C700, C750, and C800 are found at the start of regime I, which is characteristic for a developed initial porosity and a more complete carbonization.

At this stage, we may conclude that 700 °C is probably the lowest carbonization temperature for coconut shells to obtain a well developed microporosity.

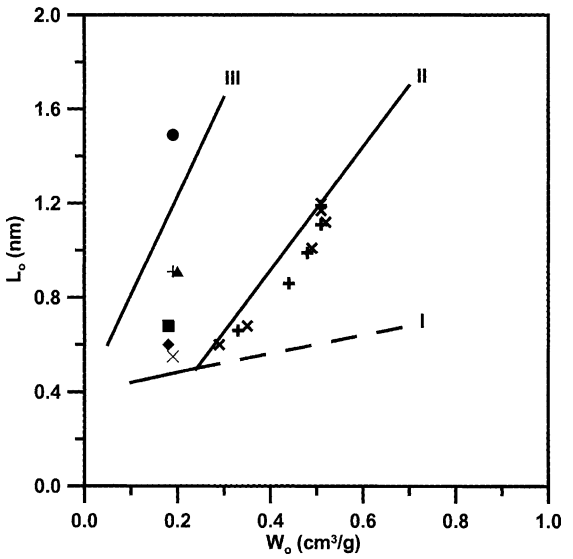

Fig. 2. The evolution of L_0 with W_0 (N_2 −196 °C): lines I, II or III correspond to specific regimes discussed elsewhere [21]. (C550 ●) (C600 ▲) (C650 +) (C700 ■) (C750 ◆) (C800 ×) (1-A-650 +) (1-A-800 ×).

4.2. Influence of the IHTT on the properties of the activated carbons

As shown in Table 3, the 1-h activation following the one- and two-step procedures with various IHTTs, leads to carbons with similar microporous properties.

The main difference between the different approaches lies in the overall burn-off (the mass loss, relative to the carbonized material, expressed in %). This quantity tends to decrease with increasing IHTT. For the carbons resulting from the one-step procedure, it drops from 26% to 14% as the IHTT treatment is increased from 550 to 800 °C. For the two-step procedure, one observes a somewhat smaller decrease, namely from 19% to 14%.

After one hour of activation, whatever procedure is followed, the sum of the mass losses (in carbonization and in activation) is 80% with respect to the initial mass of the coconut shell. Nevertheless, it would appear that for all samples prepared at low IHTTs, the porosity is still underdeveloped, as the heat flow of the activation was not sufficient to develop it. This may be the cause of the delay in activation observed for short activation times. Furthermore, the amount of tars deposited in the cooled materials is more important. It is likely that steam first eliminates these materials, which slows down the process of activation of the carbon itself. This is suggested by the fact that the rate of the C–H_2O reaction depends on the type of char. During activation, the comparison of the yields in Table 2 and the burn-offs in Table 3 shows that the mass loss is more important for chars resulting from low IHTTs, which suggests the removal of volatile materials, as well as the oxidation of the carbon.

Table 4 gives the structural characteristics of the carbons obtained by activating chars C650 and C800 between 60 and 270 min. Up to 165 min, the micropore volumes W_0 of the carbons obtained from C650 are superior to those of series C800. However, beyond this activation time, both series have similar volumes, up to a limit of 0.51 cm^3/g, but with different degrees of burn-off. The same observation applies to the average micropore width L_0, which reaches a maximum value of 1.2 nm with different degrees of burn-off. This behavior is consistent with the results of Table 3 (activation times of 60 min). This is also illustrated by Fig. 3, which shows the evolution of the PSDs of chars C650 and C800, and the corresponding activated carbons 1-650-A-60 and 1-800-A-60.

Figs. 4 and 5 show, respectively, the evolution of W_0 and L_0 in the carbons derived from chars C650 and C800 as a function of burn-off. It appears that, up to a burn-off of 50%, both W_0 and L_0 are somewhat higher in series C800 than in series C650. This is probably due to the fact that carbonization was incomplete in char C650. As shown in Fig. 2, these results correspond to the so-called regime II discussed by Stoeckli et al. [21], which is a characteristic of lignocellulosic materials.

Table 3
Main characteristics of the activated carbons resulting from the one- and the two-step procedures (soaking time 60 min)

Sample	Burn-off (%)	E_0 (kJ/mol) (N_2)	L_0 (nm) (N_2)	W_0 (cm^3/g)	W_t (cm^3/g)	S_e (m^2/g)
1-550-A-60	25.7	28.5	0.63	0.32	0.35	24.2
1-600-A-60	19.9	29.1	0.61	0.31	0.34	22.1
1-650-A-60	26.3	27.8	0.66	0.33	0.35	9.5
1-700-A-60	19.4	29.3	0.60	0.31	0.32	10.7
1-750-A-60	18.8	30.1	0.58	0.30	0.32	15.0
1-800-A-60	14	29.5	0.60	0.29	0.31	7.7
2-550-A-60	18.9	30.2	0.57	0.29	0.31	0.9
2-600-A-60	17.7	29.7	0.59	0.30	0.33	13.1
2-650-A-60	15.1	30.3	0.57	0.29	0.31	7.8
2-700-A-60	18.9	28.1	0.65	0.33	0.36	21.4
2-750-A-60	13.4	30.1	0.58	0.30	0.32	16.3
2-800-A-60	14	29.7	0.59	0.30	0.32	13.9

Table 4
Characteristics of carbons resulting from different activation times (between 60 and 270 min) at two IHTTs (650 and 800 °C)

Sample	Burn-off (%)	E_0 (kJ/mol) (N_2)	L_0 (nm) (N_2)	W_0 (cm^3/g)
1-650-A-60	26.3	27.8	0.66	0.33
1-650-A-120	39.0	24.0	0.86	0.44
1-650-A-165	46.3	22.3	0.99	0.48
1-650-A-210	65.4	21.1	1.11	0.51
1-650-A-240	78.7	20.5	1.19	0.51
1-800-A-60	14.0	29.5	0.60	0.29
1-800-A-120	23.7	27.3	0.68	0.35
1-800-A-165	43.0	22.1	1.01	0.49
1-800-A-210	55.5	21.0	1.12	0.52
1-800-A-240	70.3	20.6	1.17	0.51
1-800-A-270	78.1	20.7	1.16	0.51

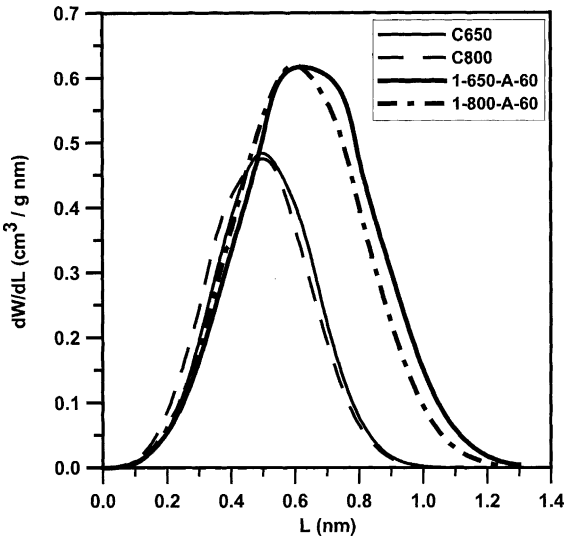

Fig. 3. Pore-size distributions (CO_2 25 °C) of carbons 1-650-A-60 (—) and 1-800-A-60 (—·—) and of the original chars, C650 (—) and C800 (– – –).

The influence of IHTT on the burn-off and on its time-dependency are discussed below (Section 4.3).

Table 5 gives the immersion calorimetry data for chars C550, C650, C700, C800 and for selected activated carbons prepared from them. The latter were chosen in order to cover the entire experimental range considered in the present study. It appears that for all samples, whatever the IHTT and activation procedures, the entire micropore

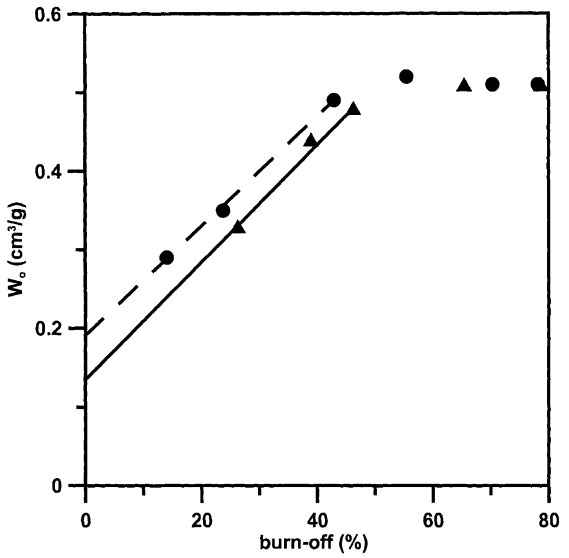

Fig. 4. The evolution of W_0 (N_2 −196 °C) with burn-off for the carbons obtained from the C650 (▲) and C800 (●) chars.

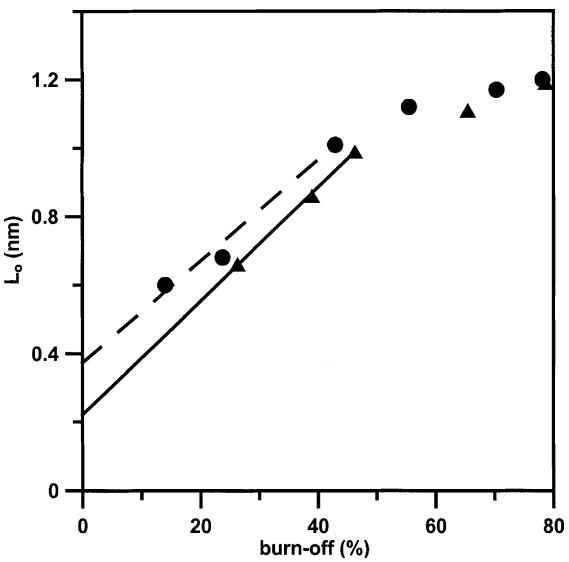

Fig. 5. The evolution of L_0 (N_2 −196 °C) with burn-off for the carbons obtained from the C650 (▲) and C800 (●) chars.

volume W_0 is accessible to CH_2Cl_2, a molecule with a diameter of approximately 0.33 nm. This is suggested by the agreement between the experimental values of $\Delta_i H$ and the values calculated from Eq. (3). On the other hand, the enthalpies of

Table 5
Data for immersion calorimetry into CH_2Cl_2 and CCl_4 at 20 °C for coconut chars prepared at different IHTTs and some activated carbons derived from them

Sample	L_0 (CO_2) (nm)	$-\Delta_i H$ calc. CH_2Cl_2 (J/g)	$-\Delta_i H$ exp. CH_2Cl_2 (J/g)	$-\Delta_i H$ calc. CCl_4 (J/g)	$-\Delta_i H$ exp. CCl_4 (J/g)	Excluded volume (CCl_4) (%)	Difference of excluded volume (1 and 2 steps) (%)
C550	0.55	80.5	79.2	76.4	77.7	0	–
1-550-A-60	0.6	127.1	124.7	120.9	109.5	9.4	
2-550-A-60	0.54	127.4	122.6	120.6	57.2	52.6	43
C650	0.48	89.2	83.2	84.4	2.7	96.9	–
1-650-A-60	0.63	138.3	132.7	130.3	110.9	14.9	
2-650-A-60	0.52	128.5	124.7	121.8	53.9	55.7	41
1-650-A-120	0.83	–	–	143.9	144.1	0	–
C700	0.53	78.7	82.4	74.6	3.2	95.8	–
1-700-A-60	0.60	125.1	128.1	118.6	86.4	27.1	
2-700-A-60	0.60	–	–	117.4	104	11.4	16
C800	0.47	83	85	–	–	–	–
1-800-A-60	0.60	133.2	123.7	126.2	91.1	27.8	
2-800-A-60	0.57	128.9	130.6	122.3	99.9	18.3	10
1-800-A-120	0.64	130.1	135.2	124.5	117.9	5.3	–

The average micropore widths L_0 have been obtained from the CO_2 adsorption isotherm at 25 °C.

immersion into CCl_4 (0.63 nm) clearly show the presence of gate effects, which depend on the history of the samples.

In the case of the chars, these results give some insight into the elementary porosity. For C550, the entire micropore volume is accessible to CCl_4. This is not the case for C650 and C700, where 96% of the volume is inaccessible to this molecule. This indicates that the elementary porosity is narrower, more homogeneous and more developed with increasing IHTT.

In the case of the carbons prepared from C550 and C650, a 60 min activation carried out in one step leads to a good accessibility of the micropore system, as the excluded volume represents only 9–15% of W_0. On the other hand, for the samples prepared in two steps and also activated for 60 min (e.g. 2-A-550-60 and 2-A-650-60), approximately 50% of the volume is no longer accessible to CCl_4. For these samples, this clearly shows that the two-stage process leads to a "gate effect".

On the other hand, for the carbons derived from C700 and C800, the same activation (60 min) leads to an exclusion of 27–28% in the one-step procedure, against 11–18% for the two-step procedure.

In comparison with the carbons based on series C550 and C650, the gate effect is somewhat larger for the one-step procedure, but it is definitely lower for the two-step procedure (the excluded volume drops from 50% to approximately 10–20% of W_0).

These observations suggest that, for the samples prepared at low IHTT, cooling to room temperature in the two-step procedure facilitates the deposit of tar at the entrance of the initial micropore system. In comparison, at high IHTTs the two-step procedure yields more homogeneous activated carbons with a well developed microporosity.

4.3. Burn-off in relation to time and IHTT

As shown in Fig. 6, the study of the burn-off as a function of time and IHTT reveals interesting patterns for the carbons prepared in the present study. We choose the limiting cases of series 1-650-A and 1-800-A activated between 60 and 270 min.

It appears that the burn-off follows two regimes, first with a gradient of $3.5\%/\min^{1/2}$ and subsequently $12\%/\min^{1/2}$. For the lower IHTT (650 °C), the first regime begins practically with activation, which means that disorganized material

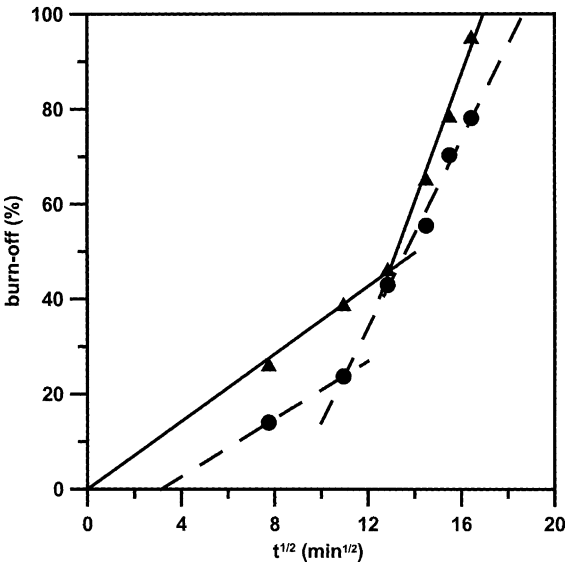

Fig. 6. The evolution of burn-off with time and IHTT for the carbons obtained from the C650 (▲) and C800 (●) chars.

is burnt-out from the start. This is followed by a change at a burn-off of approximately 45%.

On the other hand, IHTT at 800 °C leads to an induction time of approximately 10 min and the change to the second regime occurs already for a burn-off around 20%.

A comparison of Fig. 6 with Fig. 4 suggests that the second regime in the burn-off corresponds closely to the plateau observed for the increase in the micropore volume W_0 beyond a burn-off of 40–50%. At this stage, matter and voids are eliminated simultaneously and the development of porosity stops at $W_0 \sim 0.50$ cm^3/g and $L_0 \sim 1.2$ nm for the carbons resulting from the one- and two-step procedures used in the present study.

5. Conclusions

The present study shows that chars obtained by carbonizing coconut shells at low IHTTs present an underdeveloped porosity, with tars deposited at the entrance of the initial micropore system. These materials may be the cause of the delay in activation observed for short activation times.

It appears that the activated carbons obtained from coconut shells can be optimized by carbonizing above 700 °C and cooling down to room temperature, before proceeding with activation.

Furthermore, the enthalpies of immersion into CCl_4 clearly show the presence of "gate effects", which depend on the number of steps in the carbonization/activation procedure. Thus, the one-step procedure with IHTT carbonization beyond 700 °C leads to a more important gate effect than the two-step procedure. Consequently, in the case of coconut shells subjected to high IHTT, the two-step procedure leads to more homogeneous activated carbons with a well developed microporosity even at low burn-off.

Acknowledgements

The authors wish to thank Air Liquide (France) for their financial support (contract 751502/00).

References

[1] T. Wigmans, Carbon 27 (1989) 13–22.
[2] F. Rodriguez-Reinoso, J. de D. Lopez-Gonzalez, C. Berenguer, Carbon 22 (1984) 13–18.
[3] K. Gergova, N. Petrov, V. Minkova, J. Chem. Biotechnol. 56 (1993) 77–82.
[4] A.A. Attia, Adsorption Sci. Technol. 15 (1997) 707–715.
[5] M.T. Gonzalez, M. Molina-Sabio, F. Rodriguez-Reinoso, Carbon 32 (1994) 1407–1413.
[6] W.M.A.W. Daud, W.S.W. Ali, M.Z. Sulaiman, Carbon 38 (2000) 1925–1932.
[7] R. Bansal, J.B. Donnet, F. Stoeckli, Active Carbons, Marcel Dekker, New York, 1988, pp. 119–162.
[8] F. Stoeckli, in: J. Patrick (Ed.), Porosity in Carbons—Characterization and Applications, Arnold, London, 1995, pp. 67–92.
[9] M.M. Dubinin, Carbon 23 (1985) 373–380.
[10] M.M. Dubinin, Carbon 27 (1988) 457–476.
[11] G. Wood, Carbon 39 (2001) 343–356.
[12] A. Guillot, S. Follin, L. Poujardieu, in: B. McEnaney (Ed.), Characterization of Porous Solids IV, The Royal Society of Chemistry, Cambridge, 1997, pp. 573–580.
[13] F. Stoeckli, A. Guillot, D. Hugi-Cleary, A. Slasli, Carbon 38 (2000) 938–941.
[14] F. Stoeckli, A. Guillot, D. Hugi-Cleary, A. Slasli, Carbon 40 (2002) 383–388.
[15] J.S. Gregg, K.S.W. Sing, Adsorption, Surface Area and Porosity, Academic Press, London, 1982, pp. 90–110.
[16] P.J.M. Carrott, M.M.L. Ribeiro-Carrott, Carbon 37 (1999) 647–656.
[17] F. Stoeckli, A. Slasli, D. Hugi-Cleary, A. Guillot, Micropor. Mesopor. Mater. 51 (2002) 197–202.

[18] E. Fernandez, T.A. Centeno, F. Stoeckli, Adsorption Sci. Technol. 19 (2001) 645–653.
[19] F. Stoeckli, M.V. López-Ramón, D. Hugi-Cleary, A. Guillot, Carbon 39 (2001) 1115–1116.
[20] A. Guillot, F. Stoeckli, Y. Bauguil, Adsorption Sci. Technol. 18 (2000) 1–14.
[21] F. Stoeckli, E. Daguerre, A. Guillot, Carbon 37 (1999) 2075–2077.